# Ultrahigh-Pressure Liquid Chromatography: Fundamental Aspects of Compression and Decompression Heating

**R.K. Gilpin*** and **W. Zhou**
Brehm Research Laboratory, University Park, Wright State University, Fairborn, OH 45324-2031

## Abstract

**Ultrahigh-pressure liquid chromatography is an emerging technique for carrying out rapid and highly efficient separations. Unfortunately, one of the simplifying assumptions made in conventional high-performance liquid chromatography, incompressibility of the mobile phase, is not valid when higher and higher pressures are used. Rather, both compression and decompression of the eluent must be considered in terms of both heating and changes in the solvent's structure. The first of these problems, eluent heating during the compression and decompression cycles, which occurs in the pump and column, respectively, are considered in terms of a combined first principle-empirical approach that is solved (i.e., an analytic solution obtained from the resulting integral equation) using 0.01 Bar pressure steps. The approach is used to estimate compression and decompression heating for methanol and water.**

## Introduction

With the advent of modern synthetic procedures, especially those where combinatorial techniques are being used to produce large numbers of compounds in relatively short periods of time, greater and greater demands are being placed on the analytical methods for screening them. Although a variety of approaches are being used, many of them involve some form of separation technique and of these, as has been the general trend for many years, the front-line approach continues to be liquid chromatography as the result of its greater overall flexibility, scalability, and ruggedness (1–4). The current trend in many analytical laboratories is the increasing use of rapid and highly automated methods that can handle the higher sample throughput demands.

Although it is sometimes difficult to define the exact point where classical high-performance liquid chromatographic (HPLC) approaches end and faster HPLC procedures begin, the basic strategy of all modern high throughput methods is to improve chromatographic efficiency to a point where more rapid separation conditions can be used to assay dozens of samples in the same amount of time in which only a few could have been assayed previously. This has been made possible by newer higher efficiency columns constructed using either nonporous, porous non-reticulated, or porous reticulated materials that improve the eluent's flow patterns and hence the transfer kinetics of the analytes. By employing shorter forms of these types of columns packed (i.e., < 100 mm in length) in combination with hardware that can be operated at higher pressures, separations can be carried out in seconds, compared to minutes or hours.

Although the general concept of rapid HPLC using shorter columns in combination with increased eluent velocities is not new, but one that is now approximately thirty years old (5–7), an important and more recent refinement has been the use of greater than 300 Bar operating pressures in combination with sub-2 µm packings (8–22). This newer high efficiency form of separation is referred to as ultrahigh-pressure/performance liquid chromatography (UHPLC). Currently, the state-of-the-art of commercially available instrumentation extends the operating pressure range up to approximately 1000 Bar; however, custom assembled equipment allows even higher operating pressures to be used (10). With the introduction of ultrahigh-pressure liquid chromatography, mixtures with greater complexity, such as plant extract, fermentation broths, and combinatorial products, can be assayed quickly using columns packed with sub-2 µm materials.

Like many of the other refinements that are occurring in the field of liquid chromatography, the use of very high pressures to carry out separations also is not new, but one that dates back nearly four decades (23). However, these earlier applications were not successful due to the lack of available high efficiency column packings, and developments in this area were dormant for many years. This has changed within the last decade with the commercial introduction of newer types of ultrahigh efficiency separation media and equipment capable of using them at much higher operating pressures. However, with the emerging use of UHPLC, new challenges and potential problems have been introduced in

* Author to whom correspondence should be addressed: email roger.gilpin@wright.edu.

terms of separation design and chromatographic reproducibility due to eluent compressibility and expansion effects (24–26).

In conventional HPLC, one of the assumptions made for simplifying the fundamental treatment of solute migration is the incompressibility of the eluent. For moderate pressures up to approximately 250 to 300 Bar, this approximation is reasonable because only about 2% or less occurs and the resulting physicochemical changes due to compression and expansion of the eluent can be ignored. Hence, for all practical purposes, retention factors measured at one flow rate (i.e., pressure) are identical to those obtained at a different flow rate (i.e., pressure). However, when higher and higher pressures are used, compression and decompression effects can no longer be ignored. Unfortunately, a number of investigators appear to be unaware or do not understand fully the complex nature of the physicochemical changes that occur at ultrahigh pressures both in terms of (*i*) heating as the eluent is first compressed and then decompressed, and (*ii*) structural changes within the eluent. Although both of these influence the equilibria that govern solute migration, only heating resulting from compression and decompression will be considered in the current manuscript.

## Compression Heating

In carrying out liquid chromatographic separations at ultrahigh pressures, the first physical change that must be considered is eluent heating in the pumping system due to fluid compression. In attempting to model this problem, it should be recognized that the amount of compression heating is highly solvent dependent and difficult to predict using purely first principles due to the: (*i*) nonideal nature of the liquid state compared to the gas state; (*ii*) lack of needed physical data, especially for mixed and less common solvents, like many of those used in LC; and (*iii*) nonreversible heat losses. Recognizing these problems, the current manuscript attempts to address some of these limitations using a combined first principles-empirical approach to reduce differences between the amount of heating predicted and what is experimentally observed. Unfortunately, this approach does not address problems related to the lack of physical data. Nevertheless, it should be useful once these data are measured.

Although under actual UHPLC conditions some heat losses occur as the eluent is compressed in the pumping system, from a modeling approach this loss is often considered to be small and is ignored (24,25), especially after the system has been operated for a few minutes and the pump head has reached thermal equilibrium with the eluent. By doing this, the fluid compression is treated as reversible and adiabatic, and the change in temperature of the eluent with respect to a change in its pressure (i.e., dT/dP) can be estimated using equation 1, where $C_p$ is its heat capacity, $\alpha$ its thermal compression/expansion coefficient, V its molar volume, and T its initial temperature in K as it enters the pump.

$$(dT/dP)_S = \alpha TV/C_p \qquad \text{Eq. 1}$$

Previously, the problem of compression heating has been estimated for methanol (24) using the previously mentioned relationship and constant values of $C_p$, $\alpha$, and V, for a starting pressure of 1 Bar. By this approach, when pure methanol at 25°C (298.15 K) is compressed from 1 to 1001 Bar (i.e., $\Delta P$ = 1000 Bar), equation 1 predicts the eluent temperature will increase 18.1°C for V = $4.07 \times 10^{-5}$ $m^3$ $mol^{-1}$, $\alpha = 1.20 \times 10^{-3}$ $K^{-1}$, T = 298.15 K, and $C_p$ = 80.9 J $mol^{-1}$ $K^{-1}$. Whereas, this same approach predicts an increase in temperature for pure water of only 1.9°C when it is compressed from 1 to 1001 Bar, for V = $1.81 \times 10^{-5}$ $m^3$ $mol^{-1}$, $\alpha = 2.58 \times 10^{-4}$ $K^{-1}$, T = 298.15 K, $C_p$ = 75.3 J $mol^{-1}$ $K^{-1}$. Subsequently, when these estimates are compared to experimental observations, they differ significantly in some cases from the actual measured temperature changes (27).

The previously mentioned treatment is mathematically convenient and serves as a useful starting point for estimating the potential magnitude of eluent heating and differences in heating between solvents when they are compressed. However, this simplified approach overestimates the degree of heating for methanol and underestimates it for water, through the use of constant values for $C_p$, $\alpha$, and V in Equation 1 for large changes in pressure (e.g. $\Delta P$ = 1000 Bar), when these quantities are not constant but continually change throughout the compression cycle. In the cases of solvents (e.g., methanol and water) where actual experimental data are available, the relationships between $C_p$, $\alpha$, and V and pressure are neither constant nor linear, but obey more complex nonlinear relationships.

Summarized in Figures 1–2 are graphs showing the relationships between $C_p$, (lower plot), $\alpha$ (middle plot), and V (upper plot) as a function of pressure for pure methanol and water. The

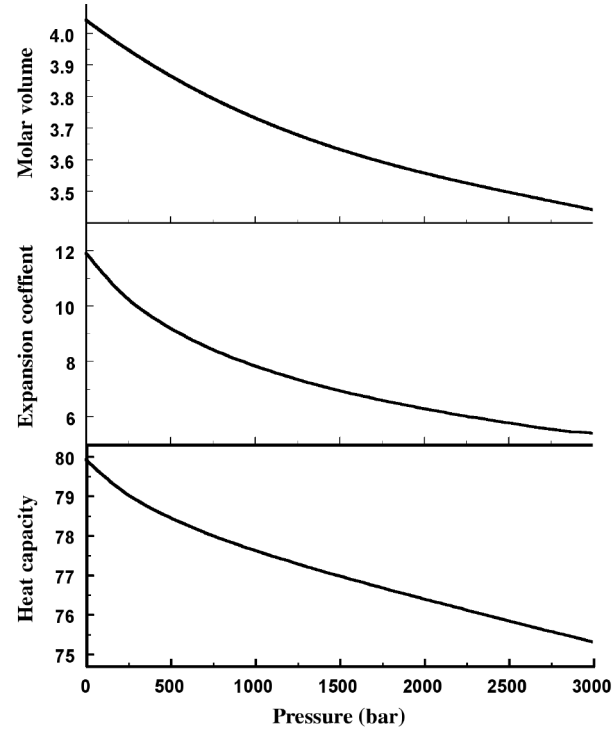


**Figure 1.** Variation of the thermodynamic properties of methanol as a function of pressure for a temperature 298.15 K. The plots from bottom to top are for the heat capacity in J/mol × K, thermal expansion coefficient in $10^{-4}$ 1/K, and molar volume given in $10^{-5}$ $m^3$/mol.

solid lines are nonlinear polynomial fits of data reported elsewhere (28,29) adjusted from closely reported temperatures to 25°C using a graphical/interpolation procedure. The resulting fits and their use are discussed later in this paper. Additional values for the heat capacity, thermal compression/expansion coefficient, and molar volume of methanol and water at other temperatures can be found in these same references. It is important to note the decreasing ($\alpha = 1.20 \times 10^{-3}$ to $7.87 \times 10^{-4}$ $K^{-1}$ for $\Delta P$ = 1000 Bar) vs. increasing ($\alpha = 2.58$ to $3.49 \times 10^{-4}$ $K^{-1}$ for $\Delta P$ = 1000 Bar) relationship between $\alpha$ and increasing pressure for methanol compared to water, which results in pronounced differences in the predicted compression heating between the two pure solvents. Compression heating is high in the case of pure methanol and low in the case of pure water.

In order to use equation 1 to predict temperature changes over large ranges of pressure, it must be rewritten in integral form (Equation 2) and solved for conditions where $C_p$, $\alpha$, and V are not constant, but are pressure dependent variables as given by equation 3.

$$\int dT = \int \alpha TV/Cp \, dP \qquad \text{Eq. 2}$$

$$\int dT = \int T f_1(P) f_2(P)/f_3(P) \, dP \qquad \text{Eq. 3}$$

Where $\alpha = f_1(P)$, $V = f_2(P)$, $Cp = f_3(P)$. In order to solve this latter relationship (equation 3), one must be able to either formulate first principle expressions for $\alpha = f_1(P)$, $V = f_2(P)$, $Cp = f_3(P)$ or use an empirical approach to obtain relationships that describe them in terms of their actual experimentally measured behaviors, which was the approach used in the current treatment.

The empirical derived relationships for $f_1(P)$, $f_2(P)$, and $f_3(P)$ were obtained via curve fitting previously published data as discussed above for the plots appearing in Figures 1 and 2. Although both the methanol and water data could be adequately fitted using third order polynomial expressions, fourth order fits were found to give slightly better R-squared values (i.e., greater than 0.999) and were used in the current treatment. In doing this, it should be noted that no physical significance is placed on these expressions other than they are accurate mathematical representations of the data given in Figures 1 and 2. As examples, the empirical relationships used to solve equation 3 for methanol were:

$$f_1(P) = 2.153 \times 10^{-13} \times P^4 - 1.615 \times 10^{-9} \times P^3 + 4.663 \times 10^{-6} \times P^2 - 7.411 \times 10^{-3} \times P + 11.98$$

$$f_2(P) = 7.554 \times 10^{-15} \times P^4 - 6.067 \times 10^{-11} \times P^3 + 2.036 \times 10^{-7} \times P^2 - 4.760 \times 10^{-4} \times P + 4.073$$

$$f_3(P) = 1.177 \times 10^{-13} \times P^4 - 8.617 \times 10^{-10} \times P^3 + 2.328 \times 10^{-06} \times P^2 - 3.956 \times 10^{-3} \times P + 80.87$$

Although not given, a similar approach was used to generate the corresponding empirical relationships for water.

Subsequently, the analytic solutions to equation 3 modified for both methanol and water were obtained using The MathWorks, Inc. (Natick, MA) MATLAB software and integrating the resulting expression for pressure steps of 0.01 Bar between each successive slice. Applying this procedure, values for compression heating for both methanol and water were calculated for a $\Delta P$ = 1000 Bar for starting pressures of 1 and 1000 Bar. For comparison purposes, the differences between the predicted compression heating obtained using constant values of $C_p$, $\alpha$, and V and equation 1 and the integration method (equation 3) and empirical fitted equations that reflect the behavior are summarized in Table I. Also included are the relative differences between the two approaches in °C and relative %. As an example, in the case of methanol, the two approaches predict an 18.1 and 13.8°C increase in temperature of the eluent, respectively, when it enters the pump at an initial temperature of 25°C and is compressed from 1 to 1001 Bar. This represents a 31.2% difference between the two predicted values.

Shown in Figure 3 are plots of the predicted temperature

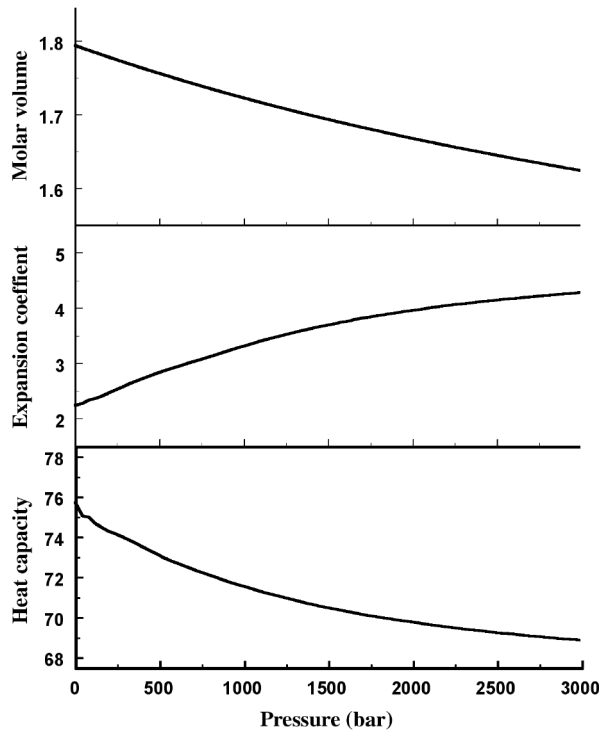


**Figure 2.** Variation of the thermodynamic properties of water as a function of pressure for a temperature of 298.15 K. The remaining labelling is the same as in Figure 1.

**Table I. Calculated Temperature Changes for Compression Heating for a Change in Pressure of 1000 Bar for Fixed (Equation 1) and Empirically Fitted (Equation 3) values of Cp, α, and V at Starting Pressures of 1 and 1000 Bar**

| | Change in Temperature (°C) $\Delta P$ = 1000 Bar and $P_i$ = 1 Bar | | | | Change in Temperature (°C) $\Delta P$ = 1000 Bar and $P_i$ = 1001 Bar | | | |
|---|---|---|---|---|---|---|---|---|
| Solvent | Eq. 1 | Eq. 3 | Diff. | % Diff. | Eq. 1 | Eq. 3 | Diff. | % Diff. |
| Methanol | 18.1 | 13.8 | 4.3 | 31.2 | 11.2 | 9.8 | 1.4 | 14.3 |
| Water | 1.9 | 2.2 | –0.3 | –13.6 | 2.5 | 2.7 | –0.2 | –7.4 |

change for the compression heating of methanol for a change in pressure of 1000 Bar (i.e., ΔP = 1000 Bar) as a function of different initial starting pressures and eluent temperatures. The curves from bottom to top are for initial eluent temperatures of 5, 15, 25, 40, and 50°C and were calculated using the integration approach and the empirical derived relationships for $C_p$, α, and V discussed previously. Similar plots for the compression heating of water are given in Figure 4 and are for the same temperatures as those shown in Figure 3. The significantly different trends between these two solvents are consistent with differences in their expansion/compression properties that are shown in the middle graphs appearing in Figures 1 and 2, respectively.

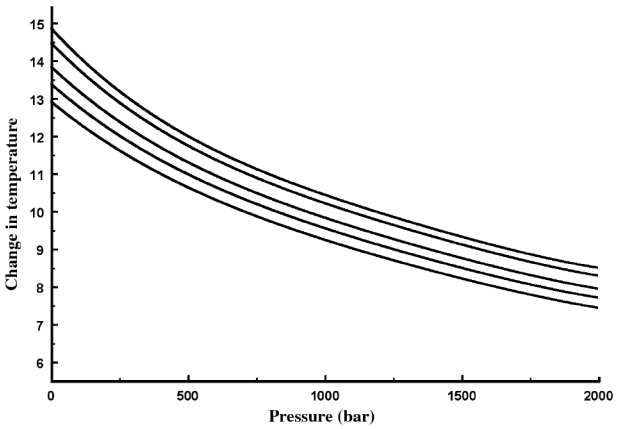


**Figure 3.** Predicted change in temperature for the compression heating of methanol vs. starting pressure for a change in pressure of 1000 Bar using the integration approach and empirically derived relationships for $C_p$, α, and V. The curves from bottom to top are for initial eluent temperatures of 5, 15, 25, 40, and 50°C.

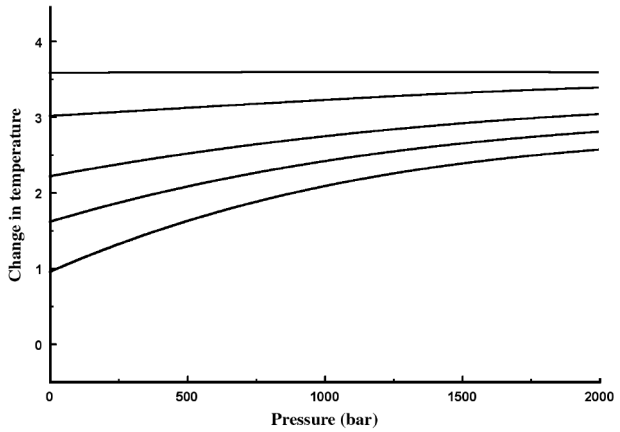


**Figure 4.** Predicted change in temperature for the compression heating of water vs. starting pressure for a change in pressure of 1000 Bar using the integration approach and the empirically derived relationships for $C_p$, α, and V. The plots appear in the same order as in Figure 3.

It is important to note that the calculated values for compression heating represent upper limits and under normal operating conditions using standard instrumentation, the increase in the eluent temperature entering the column will be less than this upper limit due to thermal losses in the pump, connecting tubing, and injection system. Furthermore, it is important to note that for both equations 1 and 3, an assumption is made that there are no entropic changes in the system (i.e., ΔS = 0) during compression. In actual practice, this is not the case and calculated values based on this assumption, irrespective of whether the fixed or the integral approach is employed, will overestimate the amount of heat produced (i.e., increase in temperature) because ΔS ≠ 0 and internal energy is stored via a change in ΔS, which is released during decompression of the eluent between the inlet and outlet of the column (i.e., conservation of energy).

## Expansion Heating

The second physical change that must be considered under UHPLC conditions is fluid decompression/expansion as the eluent travels through the packed bed. Although this change is present under normal HPLC conditions, ΔP is small enough so that any effects arising from it can be ignored. However, this is not the case in UHPLC, where the amount of heat generated due to decompression also can be a significant factor in terms of the chromatographic reproducibility. One approach that has been used to estimate decompression heating is to use the Joule-Thomson expansion of a liquid through a porous plug model. In using this approach, two assumptions are made, (*i*) the change in enthalpy for the process is zero (isenthalpic), and (*ii*) other heating due to friction can be ignored because the velocity of fluid passing though the column is relatively small (30,31). The resulting mathematical model is given in equation 4 and $C_p$, α, and V are the same quantities appearing in equation 1 earlier.

$$(dT/dP)_H = (\alpha T - 1)V/C_p \qquad \text{Eq. 4}$$

In solving the previous expression, it is important to note that the Joule-Thomson effect can be either positive or negative depending on the exact conditions with respect to the system's inversion point resulting in either heating or cooling. Under UHPLC conditions, expansion of the eluent leads to heating. The expansion heating for methanol has been estimated using equation 4 and constant values for $C_p$, α, and V as was done in the case of compression heating (24). Thus, when pure

**Table II. Calculated Temperature Changes for Expansion Heating for a Change in Pressure of –1000 Bar for Fixed (Equation 4) and Empirically Fitted (Equation 6) Values of $C_p$, α, and V at Starting Pressures of 1001 and 2000 Bar**

| | Change in Temperature (°C) ΔP = –1000 Bar and $P_i$ = 1001 Bar | | | | Change in Temperature (°C) ΔP = –1000 Bar and $P_i$ = 2000 Bar | | | |
|---|---|---|---|---|---|---|---|---|
| Solvent | Eq. 4 | Eq. 6 | Diff. | % Diff. | Eq. 4 | Eq. 6 | Diff. | %Diff. |
| Methanol | 36.5 | 35.1 | 1.4 | 4.1 | 37.5 | 37.1 | 0.4 | 1.1 |
| Water | 21.7 | 21.9 | –0.2 | –0.9 | 21.1 | 21.4 | –0.3 | –1.4 |

methanol at 25°C (298.15 K) decompresses from 1001 to 1 Bar (i.e., $\Delta P$ = 1000 Bar), V = $3.75 \times 10^{-5}$ $m^3$ $mol^{-1}$, $\alpha = 7.87 \times 10^{-4}$ $K^{-1}$, T = 298.15 K, and $C_p$ = 78.5 $mol^{-1}$ $K^{-1}$, equation 4 predicts the eluent's temperature will increase 36.5°C. This same approach predicts an increase in temperature for pure water of 21.7ºC when it is decompressed from 1001 to 1 Bar, where V = $1.74 \times 10^{-5}$ $m^3$ $mol^{-1}$, $\alpha = 3.49 \times 10^{-4}$ $K^{-1}$, T = 298.15 K, $C_p$ = 71.6 J $mol^{-1}$ $K^{-1}$.

As discussed previously for the compression heating process, the eluent's thermodynamic properties change with pressure. Thus, in order to obtain a more reliable estimate of expansion heating, equation 4 must be solved in terms of its integral form, equation 5, after making the appropriate substitutions of the empirical relationships for $f_1$ (P), $f_2$ (P), and $f_3$ (P) into equation 6.

$$\int dT = \int (\alpha T - 1) V/Cp \, dP \qquad \text{Eq. 5}$$

$$\int dT = \int (f_1 (P) T - 1) f_2 (P)/ f_3 (P) \, dP \qquad \text{Eq. 6}$$

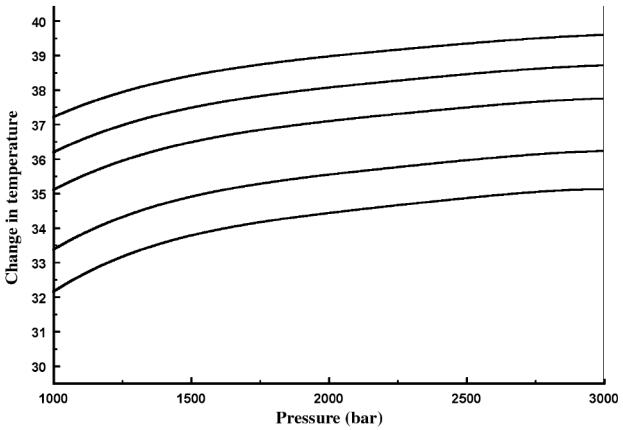


**Figure 5.** Predicted change in temperature for the expansion heating of methanol vs. starting pressure for a change in pressure of 1000 Bar using the integration approach and the empirically derived relationships for $C_p$, $\alpha$, and V. The plots appear in the reverse order as in Figure 3.

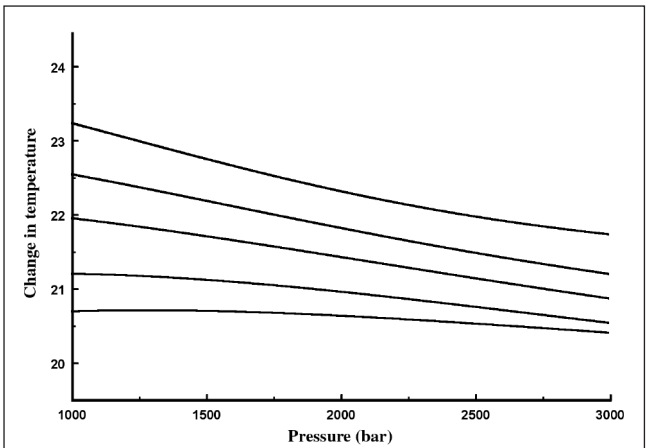


**Figure 6.** Predicted change in temperature for the expansion heating of water vs. pressure for a change in pressure of 1000 Bar using the integration approach and the empirically derived relationships for $C_p$, $\alpha$, and V. The plots appear in the reverse order as in Figure 3.

The analytic solution of equation 6 was obtained using the same software and pressure step conditions used for calculating compression heating. The resulting values for decompression heating are summarized in Table II. Also, for comparison purposes, the differences between data (i.e., in terms of both °C and relative %) obtained using constant values of $C_p$, $\alpha$, and V and equation 4 and the integration approach and empirical fitted values using equation 6 for expansion heating are summarized in Table II. Similar to the data shown in Figure 3 for compression heating, appearing in Figure 5 are plots of the predicted temperature change that results from the expansion/decompression heating of methanol for a change in pressure of 1000 Bar (i.e., $\Delta P$ = 1000 Bar) as a function of the initial starting pressure. The curves from top to bottom are for initial eluent temperatures of 5, 15, 25, 40, and 50°C. Similar plots for the decompression heating of water are given in Figure 6 and are for the same temperatures as in Figure 5. Again, as in the case of compression heating, significantly different trends between these two solvents are predicted for expansion heating.

## Conclusions

The physicochemical changes that occur under various UHPLC conditions are complex and are often difficult to describe in terms of first principles due to the nonideal nature of the liquid state compared to the gas state. Likewise, empirical models are often inadequate or incomplete due to the lack of sufficient experimental data, especially in the case of mixed solvents. Such measurements are currently in progress (27) and will be reported in a forthcoming manuscript. Nevertheless, a combination of these approaches can be useful, keeping in mind that under actual UHPLC conditions (i.e., the use of binary solvents, different compression volumes, temperatures, pressures, and nonadiabatic heat losses), the calculated values serve as only rough estimates of what to expect. Often the measured increases in temperature are significantly less than the values predicted. Likewise, with smaller bore columns and appropriate temperature control, the problem of thermal gradients in the column can be reduced.

In addition to thermal changes, a second and perhaps even more important physicochemical consideration in UHPLC is the influence of pressure on the eluent's structure, especially for mixed hydroorganic solvents (i.e., polarity changes) and the resulting changes in the equilibrium constants that govern solute migration. Although this aspect is not considered in the current paper and has received far less attention in the literature, there have been some attempts to model these effects (24–26). It is important to recognize that the elution profile of a mixture of compounds (i.e., observed using moderate pressures) can differ significantly from the elution profile of the same mixture measured at ultrahigh pressure even if an identical eluent and surface/column are used. Furthermore, the elution profile will be much less predictable as the flow rate (i.e., pressure) is changed. This effect was first reported nearly four decades ago (23) and suggests that UHPLC separations will be far more difficult to predict and reproduce than those carried out under conventional HPLC conditions (24).

## References


1. G.N. Okafo and J.K. Roberts. *Pharmaceutical Analysis*. D.C. Lee and M.L. Webb, Eds. Blackwell, Oxford, UK, 2003, Chapter 2.
2. S.P. Dixon, I.D. Pitfield and D. Perrett. Comprehensive multi-dimensional liquid chromatographic separation in biomedical and pharmaceutical analysis: a review. *Biomed. Chromatogr.* **20:** 508–529 (2006).
3. T. Hanai. Chromatography and computational chemical analysis for drug discovery. *Curr. Med. Chem.* **12:** 501–525 (2005).
4. R.K. Gilpin and C.S. Gilpin. Pharmaceuticals and related drugs. *Anal. Chem.* **79:** 4275–4293 (2007).
5. J.H. Knox. Practical aspects of LC theory. *J. Chromatogr. Sci.* **15:** 352–364 (1977).
6. R.K. Gilpin and M.H. Gaudet. Rapid high-performance liquid chromatographic determination of acetaminophen in dosage form using a totally aqueous mobile phase. *J. Chromatogr.* **248:** 160–164 (1982).
7. S. Lindsay. *High Performance Liquid Chromatography*, 2nd ed. John Wiley and Sons, London, England, 1992.
8. M.D. Jones and R.S. Plumb. The application of sub-2 µm particle liquid chromatography-operated high mobile linear velocities coupled to orthogonal accelerated time-of-flight mass spectrometry for the analysis of ranitidine and its impurities. *J. Sep. Sci.* **29:** 2409–2420 (2006).
9. O.Y. Al-Dirbashi, H.Y. Aboul-Enein, M. Jacob, K. Al-Qahtani, and M.S. Rashed. UPLC–MS–MS determination of doxazosine in human plasma. *Anal. Bioanal. Chem.* **385:** 1439–1443 (2006).
10. J.E. MacNair, K.C. Lewis, and J.W. Jorgenson. Ultrahigh-pressure reversed-phase liquid chromatography in packed capillary columns. *Anal. Chem.* **69:** 983–989 (1997).
11. N.J. Wu and R. Thompson. Fast and efficient separations using reversed phase liquid chromatography. *J. Liq. Chromatogr. Relat. Technol.* **29:** 949–988 (2006).
12. L. Nováková, L. Matysová, and P. Solich. Advantages of application of UPLC in pharmaceutical analysis. *Talanta* **68:** 908–918 (2006).
13. S.A.C Wren and P. Tchelitcheff. Use of ultra-performance liquid chromatography in pharmaceutical development. *J. Chromatogr. A* **1119:** 140–146 (2006).
14. K.A. Johnson and R. Plumb. Investigating the human metabolism of acetaminophen using UPLC and exact mass oa-TOF MS. *J. Pharm. Biomed. Anal.* **39:** 805–810 (2005).
15. J. Mensch, M. Noppe, J. Adriaensen, A. Melis, C. Mackie, P. Augustijns, and M.E. Brewster. Novel generic UPLC/MS/MS method for high throughput analysis applied to permeability assessment in early drug discovery. *J. Chromatogr. B* **847:** 182–187 (2007).
16. M. Kalovidouris, S. Michalea, N. Robola, M. Koutsopoulou, and I. Panderi. Ultra-performance liquid chromatography–tandem mass spectrometry method for the determination of lercanidipine in human plasma. *Rapid Commun. Mass Spectrom.* **20:** 2939–2946 (2006).
17. K. Yu, D. Little, R. Plumb, and B. Smith. High-throughput quantification for a drug mixture in rat plasma—a comparison of ultra-performance liquid chromatography–tandem mass spectrometry with high-performance liquid chromatography–tandem mass spectrometry. *Rapid Commun. Mass Spectrom.* **20:** 544–552 (2006).
18. G.J. Dear, A.D. James, and S. Sarda. Ultra-performance liquid chromatography coupled to linear ion trap mass spectrometry for the identification of drug metabolites in biological samples. *Rapid Commun. Mass Spectrom.* **20:** 1351–1360 (2006).
19. S. King, P.J. Stoffolano, E. Robinson, T.E. Eichhold, S.H. Hoke II, T.R. Baker, E.C. Richardson, and K.R. Wehmeyer. The evaluation and application of UPLC for the rapid analysis of dose formulations. *LC/GC N. Am.* **23(May Supplement):** 36–39 (2005).
20. L. Novakova, D. Solichova, and P. Solich. Advantages of ultra performance liquid chromatography over high-performance liquid chromatography: Comparison of different analytical approaches during analysis of diclofenac gel. *J. Sep. Sci.* **29:** 2433–2443 (2006).
21. M.E. Swartz. UPLC: An introduction and review. *J. Liq. Chromatogr. Rel. Technol.* **28:** 1253–1263 (2005).
22. D.T.T. Nguyen, D. Guillarme, S. Rudaz, and J.L. Veuthey. Fast analysis in liquid chromatography using small particle size and high pressure. *J. Sep. Sci.* **29:** 1836–1848 (2006).
23. B.A. Bidlingmeyer, R.P. Hooker, C.H. Lochmuller, and L.B. Rogers. Improved chromatographic resolution from pressure-induced changes in liquid-solid distribution. *Sep. Sci.* **4:** 439–446 (1969).
24. M. Martin and G. Guiochon. Effects of high pressure liquid chromatography. *J. Chromatogr. A* **1090:** 16–38 (2005).
25. F. Gritti and G. Guiochon. Effects of the thermal heterogeneity of the column on chromatographic results. *J. Chromatogr. A.* **1131:** 151–165 (2006).
26. NJ. Wu. Fundamental and practical aspects of ultrahigh-pressure liquid chromatography for fast separations. *J. Sep. Sci.* **30:** 1167–1182 (2007).
27. R.K. Gilpin and W. Zhou Unpublished data.
28. T. Sun, S.N. Blswas, N.J. Trappenlers, and C.A. Ten Seldam. Acoustic and thermodynamic properties of methanol from 273 to 333 K and at pressures to 280 MPa. *J. Chem. Engi. Data* **33:** 395–398 (1988).
29. W. Wagner and A. Prub. The IAPWS formulation 1995 for the thermodynamic properties of ordinary water substance for general and scientific use. *J. Phys. Chem. Ref. Data* **31(2):** 387–535 (2002).
30 W.B. Gosney. *Principles of Refrigeration*. Cambridge University Press, Cambridge, 1982, Chapter 8.
31. D.F. Eggers, N.W. Gregory, G.D. Halsey, and B.S Rabinovitch. *Physical Chemistry*. Wiley, New York, 1964, Chapter 7.


Manuscript received November 20, 2007;
revision received January 11, 2008.